

Sol–Gel Synthesis of Fluoride-Substituted Talc

Florangel Duldulao Perez and James M. Burlitch*

Department of Chemistry, Baker Laboratory, Cornell University, Ithaca, New York 14853-1301

Received March 21, 1995. Revised Manuscript Received October 3, 1995[®]

Fluoride-substituted talcs, $\text{Mg}_3\text{Si}_4\text{O}_{10}(\text{F}_x, \text{OH}_{1-x})_2$ (fluorotalcs), where x is 0.45 or 0.71, were synthesized at 750 °C at confining pressures between 150 and 200 MPa in 72 h from calcined amorphous xerogels, which were prepared from a fluoridated magnesium silicate sol. A soft, slippery product was obtained when the xerogel was fired with more than the stoichiometric amount of water necessary in the final structure. FTIR and XRD analyses showed decreases in the O–H stretching frequency and in the position of the (060) peak to lower 2θ values, respectively, with increase in x . The upper limit of the thermal stability of the synthetic fluorotalcs, estimated by thermal analysis (DTA and TG), was 1115 or 1075 °C when x was 0.45 or 0.71, respectively. The former represents an increase in thermal stability of ~ 250 °C compared to synthetic talc without fluoride. The slightly lower limit obtained for the latter may indicate that too high fluoride substitution may destabilize the structure. Attempts to synthesize phases with $x > 0.71$ resulted in mixtures of a talc phase and MgF_2 , indicating that fluoride does not fully substitute for hydroxide under the conditions used. Firing of xerogels above 800 °C under atmospheric pressure did not yield talc but formed forsterite and humite minerals including norbergite.

Introduction

Compared to metals and polymers, advanced ceramics exhibit the desirable properties of high-temperature strength, high wear resistance (being harder than metals), and chemical stability in erosive wear applications. However, unlike metals that exhibit ductile behavior, ceramics are brittle and may fail from localized high impact loading. To increase the toughness of ceramics, composites have been fabricated in which the ceramic matrix is reinforced by ceramic fibers 10–30 μm in diameter that have a high modulus. Prevention of catastrophic failure of the composite structure by protection of the fibers from cracks that are propagating through the matrix in which the fibers are imbedded has been the subject of numerous studies; an important question concerns the type of interface that is necessary to provide this mechanical protection.¹ It has been suggested that modification of the interface between fiber and matrix is necessary to achieve high fracture toughness in these fiber-reinforced ceramic matrix composites (CMCs).^{2–5} For instance, high fracture toughness in alkali or alkaline earth aluminosilicate glass ceramics that were reinforced with SiC fibers has been associated with the formation of a carbon-rich interface formed during processing.^{6,7} However, rapid oxidation of this carbon interface is observed when the CMC is exposed to air at 900 °C, even for a short time, resulting in the embrittlement of the composite.⁸

The use of sheet silicates as interface modifiers between the fiber and the brittle ceramic matrix has been reported.^{9,10} The bonding between the octahedral and tetrahedral layers that comprise the sheets in the silicate structure is strong enough to allow the transfer of stress from the matrix to the stronger fibers. The weaker bonding between the sheets may provide a sufficiently weak interface to allow some fiber pullout, which will deflect cracks.^{3–5} As oxides, sheet silicates are inherently stable toward oxidation. Furthermore, the use of fluoridated (i.e., F substituted for OH) sheet silicates could be especially advantageous as they have relatively higher decomposition temperatures compared to the hydroxyl analogues. Improved thermal stability with increased fluoride substitution has been observed for the micas, in which the increase in the interlayer bond energy has been attributed to the removal of the repulsive forces between the proton in the –OH group and the interlayer cation.^{11,12}

Recently, we described the sol–gel synthesis of potassium fluorophlogopite ($\text{KMg}_3\text{Si}_3\text{AlO}_{10}\text{F}_2$, KFP), a sheet silicate with an interlayer charge of -1 , and demonstrated that its sol–gel precursor can be used to make coatings that convert to KFP on heating under confined conditions.¹³ That study has been extended to the synthesis of fluorotalc, $\text{Mg}_3\text{Si}_4\text{O}_{10}\text{F}_2$, a layered structure with no interlayer charge, as a potential fiber coating for CMCs. In talc, all three octahedral sites are occupied by Mg^{2+} (Figure 1).^{14,15} Because there is no net charge within the layers, the interlayer bonding in talc has been attributed to van der Waals forces,¹⁶ although calculations show that electrostatic surface energies are

* To whom correspondence should be addressed.

[®] Abstract published in *Advance ACS Abstracts*, November 15, 1995.

(1) Cooper, R. F.; Hall, P. C. *J. Am. Ceram. Soc.* **1993**, *76*, 1265–1273.

(2) Evans, A. G.; He, M. Y.; Hutchinson, J. W. *J. Am. Ceram. Soc.* **1989**, *72*, 2300–2303.

(3) Kerans, R. J.; Hay, R. S.; Pagano, N. J.; Parthasarathy, T. A. *Ceram. Bull.* **1989**, *68*, 429–442.

(4) Marshall, D. B. *J. Am. Ceram. Soc.* **1984**, *67*, C259.

(5) Marshall, D. B.; Evans, A. G. *J. Am. Ceram. Soc.* **1985**, *68*, 225–231.

(6) Bonney, L. A.; Cooper, R. F. *J. Am. Ceram. Soc.* **1990**, *73*, 2916–2921.

(7) Cooper, R. F.; Chyung, K. *J. Mater. Sci.* **1987**, *22*(9), 3148–3160.

(8) Cranmer, D. C. *Ceram. Bull.* **1989**, *68*, 415–419.

(9) Beall, G. H.; Chyung, K.; Dawes, S. B.; Gadkaree, K. P.; Hoda, S. N. U. S. Patent 4,935,387, 1990, and U.S. Patent 4,948,758, 1990.

(10) Chyung, K.; Dawes, S. B. *Mater. Sci. Eng.* **1993**, *A162*, 27–33.

(11) Giese, R. F. *Z. Kristallogr.* **1975**, *141*, 138–144.

(12) Zlobik, A. B. In *Kirk-Othmer Encycl. Chem. Technol.*, 3rd ed.; 1981, pp 414–439.

(13) Duldulao, F. D.; Burlitch, J. M. *Chem. Mater.* **1993**, *5*, 1037.

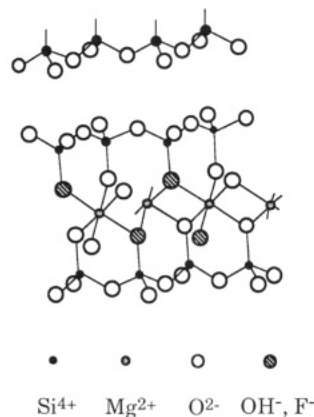


Figure 1. Idealized sketch of a portion of the crystal structure of fluorotalc.

not negligible.¹⁷ Weak attraction between the layers gives talc its characteristic properties (soft and slippery) and enables its use as a solid lubricant. As an interface modifier, fluorotalc ought to provide a weaker bond than KFP.

The substitution of hydroxide ion by fluoride ion in the octahedral layer has been known to occur naturally in talc; as much as 45% F substitution has been found in rare specimens.¹⁸ Hydrothermal synthesis of talc with F substitution of up to 60% has been reported.¹⁹ Van Valkenburg reported the hydrothermal synthesis of talc with up to 50 mol % fluoride substitution from stoichiometric proportions of MgO, SiO₂, and MgF₂ in the temperature range 400–800 °C and pressures of 110–138 MPa.²⁰ An increase in the thermal decomposition temperature by 180 °C was attributed to the substitution of fluoride for hydroxide.

Since partial fluoride substitution increased the thermal stability of talc, it seemed reasonable to presume that additional stability would accompany even higher substitution. A synthesis method was sought that would permit the fluorotalc to be coated onto fibers either as the precursor or as a slurry of a very fine powder. Sol-gel methods allow the mixing of necessary components at the molecular level through the use of solution precursors. The synthesis technique described in this paper uses a single-sol precursor to fluorotalc, obtained by modification of the peroxide-assisted synthesis of fluoridated magnesium silicate xerogels recently developed in our laboratory.^{13,21} Firing of the resulting xerogels at high pressure produced talc with up to 71% F substitution, one of the highest levels ever achieved. The soft, flaky products that were produced in the presence of excess water contrasted with the somewhat harder products formed by a diphasic sol-gel method.^{22–24}

(14) Radoslovich, E. W. *Nature* **1961**, *191*, 67–68.

(15) Gruner, J. W. Z. *Kristallogr.* **1934**, *88*, 412–419.

(16) Ward, W.; Phillips, J. M. *Surf. Sci.* **1971**, *25*, 379–384.

(17) Giese, R. F. *J. Clays Clay Miner.* **1975**, *23*, 165–166.

(18) Abercrombie, H. J.; Skippen, G. B.; Marshall, D. D. *Contrib. Mineral Petrol.* **1987**, *97*, 305–312.

(19) Duffy, C. J.; Greenwood, H. J. *Am. Miner.* **1979**, *64*, 1156–1174.

(20) Van Valkenburg, A. Jr. *J. Res. Natl. Bur. Standards* **1955**, *55*(4), 215–217.

(21) Duldulao, F. D.; Burlitch, J. M. *Chem. Mater.* **1991**, *3*(5), 772–775.

(22) Rywak, A. A.; Burlitch, J. M. *Eos. Trans. AGU* **1993**, *74*(16), 165–166.

(23) Rywak, A. A. Ph.D. Thesis, Cornell University, 1994.

(24) Rywak, A. A.; Burlitch, J. M., submitted for publication.

Experimental Section

General Comments. All precursor synthesis operations were carried out under a dry argon atmosphere unless otherwise noted.²⁵ Reagent-grade methanol was twice distilled from magnesium methoxide. TEOS (99+%), hydrogen peroxide (30%), and deuterated water were obtained from Aldrich Chemical Co. Magnesium chips (99.99%) were obtained from Alfa Chemicals. Aqueous HF (analyzed to be 48.8%) was obtained from Mallinckrodt. Silver tubing (99.9%; 6.35 mm o.d. × 5.84 mm i.d. × 10 cm long) for high-pressure syntheses was obtained from Johnson Matthey Electronics.

High-pressure synthesis operations were carried out in a Leco Tem-Pres apparatus, which consisted of a MRA-138R vessel connected to a IHY-6026 gauge assembly. The vessel was heated in a vertically oriented tube furnace controlled by an Omega Engineering Model CN 1200 series controller. The temperature of the vessel wall was monitored separately by a thermocouple connected to an Omega digital thermometer. Temperatures quoted are those of the vessel's wall.

A Mattson FTIR GL-1040 spectrometer was used to record spectra (4 cm⁻¹ resolution) of powders as pellets with dry KBr. KBr disks were used as the reference. XRD powder patterns were recorded using a Scintag PAD V diffractometer. Routine scans of powders in a quartz, low background holder were performed at 3–5°/min and chopper increment of 0.03. Si powder was used as an internal standard to accurately determine the position of the (060) peak; the scan rate was 0.75–1.5°/min. At least four values for *d*(060) were averaged.

Thermal analysis was carried out on a Seiko Instruments TG/DTA 320 analyzer. Powders were packed loosely into platinum pans by lightly tapping and were heated to the desired temperature at 10 °C/min in a flow of N₂ (250 mL/min) dried by passing through a column of Aquasorb (Mallinckrodt). α-Al₂O₃ was used as reference.

²⁹Si MASS NMR spectra were obtained using a Bruker AF300 spectrometer with a DOTY MASS probe; samples were packed in a sapphire rotor with Vespel end caps. The spinning rate was 4 kHz.

Analysis of fluoride ion concentration was performed using an Orion Research Model 701A digital ionalyzer with Orion Research Model 96-09 combination fluoride electrode. Samples in Ni crucibles were digested in NaOH flux at 600 °C for 30 min; the procedure²⁶ was scaled down for samples under 100 mg. Microprobe WDS analyses were carried out using a JEOL Superprobe 733, Tracor Northern 5500. The samples were cold-mounted in epoxy resin and were polished with ~0.05 μm alumina prior to being coated with carbon.

A Hewlett-Packard 5880A gas chromatograph equipped with a 25 m cross-linked, methylsilicone, capillary column and a flame ionization detector was used to analyze ether solutions of head-space vapors above the sol.²⁷

Preparation of Precursors. The following procedure describes the synthesis of a precursor to fluorotalc with nominally 75% fluoride substitution. A 250 mL Schlenk reaction vessel (SRV) containing about 100 mL of MeOH and a magnetic stir bar was charged with Mg chips (0.2516 g, 0.010 35 mol). The SRV was placed in an ice bath and was equipped with a water-cooled condenser and a three-way gas adapter. The mixture was stirred under a slow flow of Ar. Vigorous gas evolution was observed until all of the Mg had reacted. The colorless, nearly clear Mg(OMe)₂ solution was quantitatively filtered (D-porosity frit) into a 250 mL addition funnel.

TEOS (2.8479 g, 0.013 69 mol) was transferred quantitatively via a cannula to the stirred Mg(OMe)₂ solution to obtain a clear, colorless solution. The addition funnel that contained the solution of alkoxides was attached to a creased, 500 mL three-necked flask charged with ~100 mL of MeOH. The flask was previously equipped with a mechanical stirrer and a water-cooled condenser with a three-way gas adapter. The

(25) Burlitch, J. M. *How To Use Ace No-Air Glassware*; Ace Glass Co., Inc.: Vineland, NJ, 1984; pp 1–12.

(26) Palmer, T. A. *Talanta* **1972**, *19*, 1141–1145.

(27) Yeager, K. E.; Burlitch, J. M. *J. Non-Cryst. Solids* **1992**, *149*, 179–188.

Table 1. Synthesis Conditions for Firing of Xerogels and Products Identified by XRD^a

sample no.	calcined xerogel (g)	H ₂ O added (g)	nominal (actual) ^e %F	temp (°C)	pressure (MPa)	products ^d (from XRD)
1		0.0	50 (45)	748	162	FTc, Ag ^b
2	0.3615	0.0	75	748	165	FTc, Nob, Ag, ^b AS
3	0.3885	0.5	75 (71)	753	169	FTc
4	0.7031	0.3283	90	750	148	FTc, S
5		0.0	100	755	210	AS, Nob, Ag ^b
6	0.3953	0.4329	100	750	163	FTc, S
7 ^c	0.1665	0.0939	100	750	148	FTc, S

^a Firing conditions: 750 °C, 72 h. ^b From Ag tubing used to contain the powder. ^c 4.7 wt % natural (hydroxy) talc used as seed crystals. ^d FTc = fluorotalc; Nob = norbergite (Mg₂SiO₄·MgF₂); S = sellaite (MgF₂), AS = amorphous solid. ^e Ion selective potentiometry.

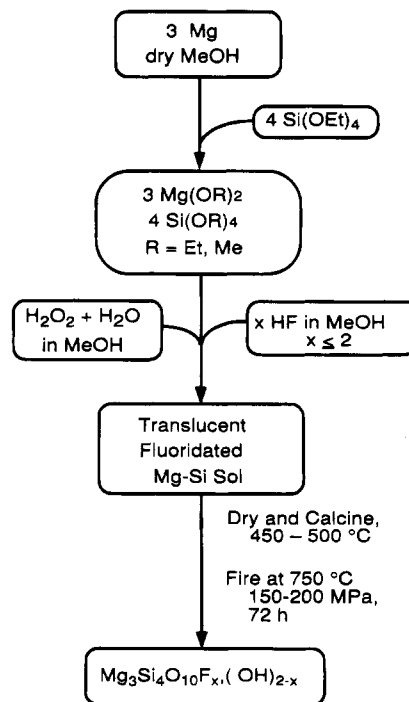
contents of the addition funnel were transferred into the creased flask, and the funnel was replaced with a rubber septum.

A solution of hydrogen peroxide (0.1677 g, 0.001 48 mol of H₂O₂) and distilled, deionized water (0.4635 g, 0.025 75 mol) were withdrawn from a Nalgene beaker into a 60 mL plastic syringe containing ~40 mL of MeOH. The syringe needle was attached to a cannula using a thin polyethylene tube, and the cannula was inserted into the reaction vessel through the septum. Similarly, 0.2134 g (0.005 207 mol) of 48.8% aqueous HF was withdrawn from a polyethylene dropper bottle through a polyethylene needle into a second 60 mL plastic syringe containing MeOH (~40 mL). The needle was inserted through the septum by means of a short, larger gauge, steel needle passed through beforehand. Then the steel needle was withdrawn. Using a syringe pump, the solutions of H₂O₂ and HF were simultaneously added at the rate of 0.15 mL/min to the vigorously stirred solution of alkoxides. The clear and colorless sol obtained was stirred until GC analysis²⁷ of the head space above the sol showed no peak due to TMOS (typically within 24 h of sol preparation).

Working in the air, the sol was concentrated with a rotary evaporator at reduced pressure. To reduce drying time, the thin, colorless slurry so obtained was dried with a heat lamp in a 1 L polyethylene beaker that was loosely covered with a watch glass. To reduce residual carbon, the resulting white xerogel was ground into a powder with a mortar and pestle, then moistened with a few milliliters of 30% H₂O₂, and dried under a heat lamp for several hours. When dry, a portion of the xerogel (1.03 g) was placed in an alumina boat, and was calcined in a tube furnace at 450 °C for 12 h (the ramp rate was 25 °C/h) under an atmosphere of dry air or O₂. The calcined xerogel was very light gray.

Firing at High Pressure. After having one end closed by a TIG welder, a silver tube was charged with the calcined xerogel and with H₂O (see Table 1). In some experiments, natural talc (Aldrich) was mixed thoroughly with the calcined xerogel by grinding lightly in an agate mortar and pestle prior to loading into the tube. While the tube was partly immersed in cold water, the open end was welded shut. The tube was inserted into the high-pressure vessel, and D₂O was added. Heavy water was used to check for leaks in the silver tubes. The vessel was sealed and was heated to the desired final temperature at a ramp rate of 100 °C/h and held for 72 h. The final pressure (e.g., 169 MPa, 24 500 psi for **3**), was provided by the supercritical D₂O. The pale, gray product, **3**, was removed from the tube, and was dried under vacuum at 180 °C for at least 10 h. Anal. Calcd for Mg₃Si₄O₁₀(F_{0.71},OH_{0.29})₂: F, 7.06%. Found: F, 7.03 ± 0.2%. FTIR: 3669 (vw, sharp), 3650–3173 (vw, br), 2706 (vw, sharp), 1040 (vs, b), 692 (w), 670 (sh), 521 (m, sh), 486 (s, sh), 465 (s), 426 (m, sh) cm⁻¹. XRD: *d* spacings in angstroms (rel intensity) at 9.441 87 (68), 4.692 21 (10), 4.572 05 (12), 2.616 77 (5), 2.601 76 (7), 2.587 66 (7), 2.480 14 (12), 2.466 62 (8), 2.455 32 (6), 2.232 86 (4), 1.871 43 (6), 1.631 06 (5), 1.522 95 (22), 1.515 77 (5), 1.316 17(6).

Other fluorotalc precursors with different levels of fluoride substitution were prepared by the above procedure. Details

**Figure 2.** Schematic diagram for the preparation of fluorotalc.

for other experiments that were carried out in essentially the same manner are given in Table 1.

Results and Discussion

Synthesis. The method used previously for the preparation of a magnesium silicate fluoride sol having 3Mg:3Si:2F ratio was modified for the synthesis of a stable fluorotalc (3Mg:4Si:2F) precursor sol (Figure 2).^{13,21} The slow, simultaneous addition of the hydrolysis agent (a methanolic solution of 30% H₂O₂) and the fluoridating agent (aqueous HF in methanol) to a stoichiometric solution of magnesium methoxide and tetraethyl orthosilicate (TEOS) in methanol gave a stable, nearly clear sol. Previous work showed that the presence of Mg(OMe)₂ catalyzes the in situ formation of the more reactive alkoxide, tetramethyl orthosilicate (TMOS), from the transesterification reaction of TEOS in methanol.^{27,28} The use of aqueous H₂O₂ facilitated the hydrolysis and condensation of Mg(OMe)₂ and TMOS, which would otherwise react at very different rates, and avoided precipitating a hydroxide of magnesium.^{29,30} Enough 30% H₂O₂ was added to the sol to hydrolyze one half of the alkoxide groups on magnesium and silicon.³¹ Reactions were continued until consumption of TMOS, which was monitored by GC analysis of the headspace above the sol,²⁷ was complete.

The use of aqueous HF to incorporate fluoride ions into the magnesium silicate network during the precursor preparation controls the amount of fluoride that will ultimately substitute for hydroxide in the talc structure. Since all the components are in solution, intimate mixing is achieved. Thus, all the elements necessary for the final structure are present in the precursor xerogel prior to firing at high pressure. Previous work

(28) Yeager, K. E.; Burlitch, J. M. *Chem. Mater.* **1991**, *3*, 387.

(29) Burlitch, J. M.; Beeman, M. L.; Riley, B.; Kohlstedt, D. L. *Chem. Mater.* **1991**, *3*, 692–698.

(30) Burlitch, J. M. U.S. Patent 5,019,293, 1991.

(31) The amount of "H" from 30% H₂O₂ was calculated by assuming that two protons are provided by H₂O₂ and one proton by H₂O.

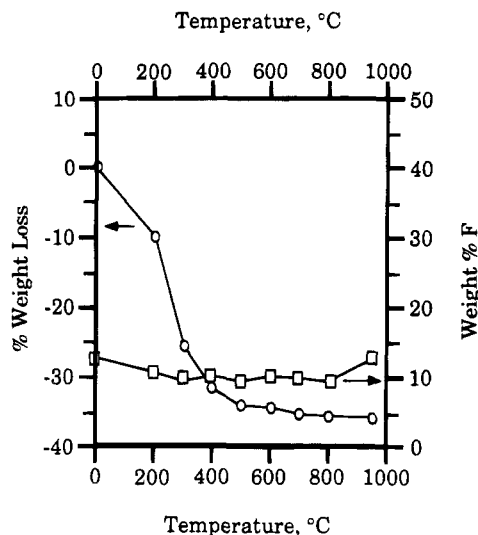


Figure 3. Change in mass (circles) and in % F content (squares) during calcination of the xerogel for nominally 100% F-substituted talc. The calculated fluoride content was corrected for the amount of calcinable material in the xerogel.

on the incorporation of fluoride ions into talc used complex fluoride buffers (graphite–methane–wollastonite–fluorite–quartz) to fix the ratio of $f_{\text{H}_2\text{O}}/f_{\text{HF}}$.^{19,32} A hydrothermal synthesis of partially substituted fluorotalc from SiO_2 , MgO , and MgF_2 needed mechanical grinding to ensure good mixing.²⁰

To aid in the removal of carbonaceous products, the dried xerogel was treated with aqueous H_2O_2 . The peroxide may act as combustion aid,³³ and the additional water it provides may promote further hydrolysis and condensation reactions and the removal of organic ligands as alcohols. To determine the optimum calcination conditions, the change in mass and in the fluoride content²⁶ of the xerogel, nominally having 100% F substitution, was monitored as a function of temperature. As shown in Figure 3, weight loss in a stream of dry air was essentially complete at 500 °C, while the fluoride content, corrected for the amount of calcinable material in the xerogel, remained stoichiometric within experimental error. XRD analysis showed that the xerogel remained amorphous up to 500 °C. Thus, precursors were calcined at 450–500 °C prior to firing at higher temperatures and pressures. In some experiments, water was added as a mineralizer to the calcined xerogels prior to the high-pressure treatment.

XRD analysis showed that xerogels fired above 800 °C at atmospheric pressure did not yield talc but formed forsterite³⁴ (Mg_2SiO_4) and humite minerals that include norbergite.³⁵ Seeding the xerogel with natural talc and firing under the same conditions gave the same results. XRD and ²⁹Si NMR analyses indicated that the talc seeds decomposed.

Phase Identification and Characterization. Table 1 shows the firing conditions and products from precursors of varying fluoride content. Fluorotalc was obtained in all cases but one. Figure 4 compares representative XRD patterns from products having

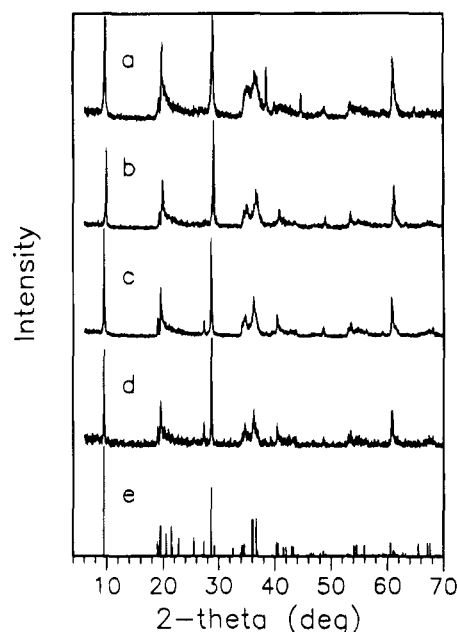


Figure 4. XRD powder patterns of high pressure products from talc xerogels with varying (target) degrees of F substitution: (a) **1** (50), (b) **3** (75), (c) **4** (90), (d) 100% compared with the calculated XRD pattern of talc (e).

different percentages of fluoride substitution, with the calculated XRD pattern for talc.^{15,36} XRD analysis of two products, viz., **1** from the 50% F-substituted xerogel and **3** from the 75% F-substituted xerogel with water added as mineralizer showed peaks at ~ 9.5 , 19, 20, 29, and 61° (2θ), which qualitatively match those of talc;³⁷ these XRD patterns have no extra peaks from a second silicate phase, and no broad diffraction feature between 20 and 30 °(2θ) from amorphous silicates.

Analysis of products **1** and **3**, using ion selective electrode (ISE) potentiometry, indicated that the powders contain $4.48 \pm 0.34\%$ and $7.03 \pm 0.20\%$ F, respectively. Since there were no other phases observed by XRD, it is reasonable to assume that the fluoride substitution in the talcs corresponded to $45 \pm 3\%$ and $71 \pm 2\%$, respectively. The latter value is one of the highest reported for talc.

SEM analysis of **3** shows it to be somewhat porous and composed of platelike crystallites the edges of which may be seen in the photomicrograph in Figure 5. In contrast, **1** (not shown) appeared to be more dense. Analysis of the fluoride content of **1** by wavelength-dispersive X-ray spectroscopy gave $4.4 \pm 0.5\%$ F by weight, in good agreement with the ISE result. Similar analysis of **3**, however, yielded a low fluoride content of 3.4 ± 0.01 wt %, which is attributed to the porous nature of sample.

Products from xerogels having nominal fluoride substitutions of 90% and 100% had XRD peaks that match those of MgF_2 ; peaks at ~ 27 , 40.5, and 51.5 °(2θ) were observed,³⁸ together with peaks for talc. It appears that fluoride does not fully substitute for hydroxide in the talc structure under the conditions used. Seeding the xerogel with fine, natural talc gave the same mixture of phases in the product. The IR spectrum of **7** showed

(32) Munoz, J. L.; Eugster, H. P. *Am. Miner.* **1969**, *54*, 943–959.

(33) Debsikdar, J. C. *J. Mater. Sci.* **1985**, *20*(12), 4454–4458.

(34) Morris, M. C.; McMurdie, H. F.; Evans, E. H.; Paretzkin, B.; Parker, H. S.; Pyrras, N. P.; Hubbard, C. R. *NBS Monogr.* **25** **1984**, Sect. 20, 71.

(35) Swanson, H. E.; Cook, M. I.; Evans, E. H.; deGroot, J. H. *NBS Circular* **539** **1960**, *10*, 39.

(36) Yvon, K.; Jeitschko, W.; Parthe, E. *J. Appl. Crystallogr.* **1977**, *10*, 73–74.

(37) Stephenson, D. A.; Sclar, C. B.; Smith, J. V. *Mineral. Mag.* **1966**, *35*, 838–846.

(38) Swanson, H. E.; Fuyat, R. K.; Ugrinic, G. M. *NBS Circular* **539** **1955**, 33–34.

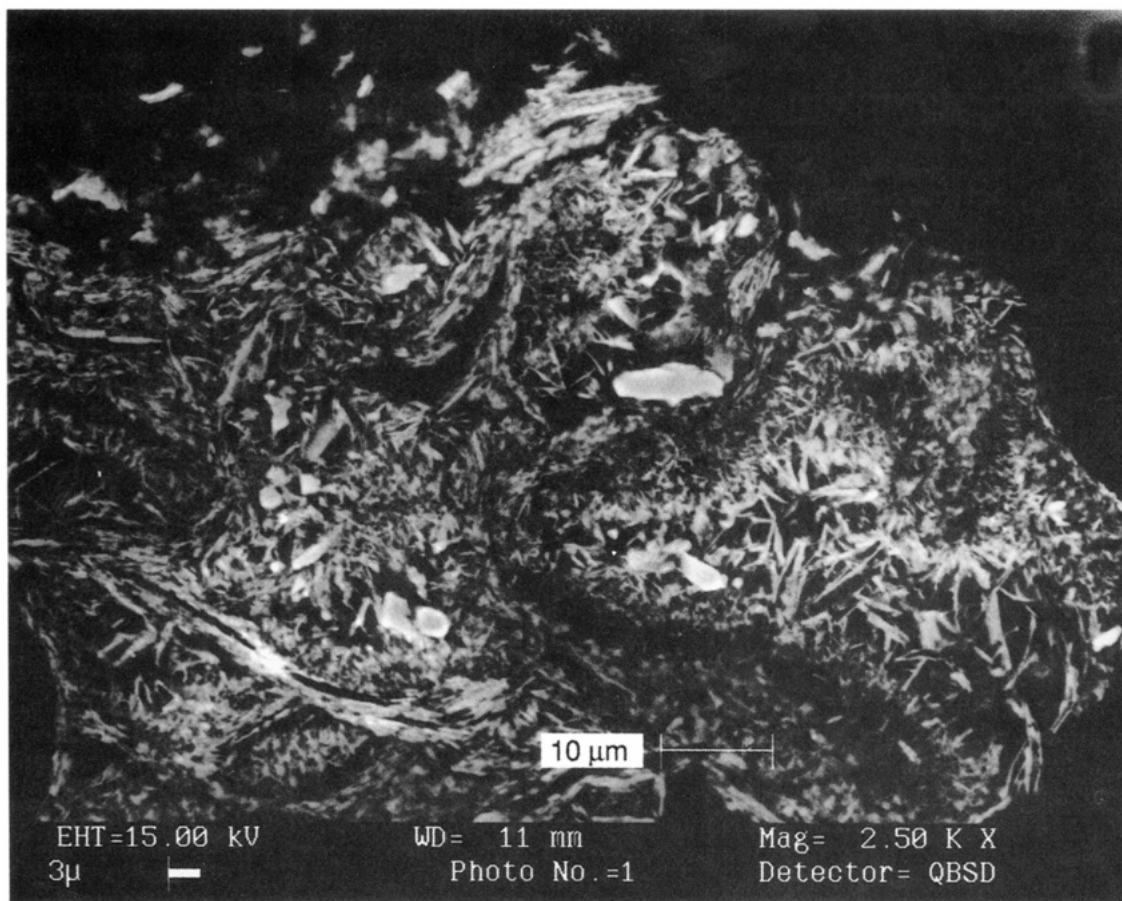


Figure 5. SEM back-scattered electron image of fluorotalc, **3** showing platelike morphology. The scale bar represents 10 μm .

only one band assigned to $\nu_{\text{O-H}}$ at 3668.6 cm^{-1} , which is 8 cm^{-1} lower than $\nu_{\text{O-H}}$ for natural talc (see below).

As shown in Figure 1, talc is composed of an octahedral layer "sandwiched" between two tetrahedral layers. Since the tetrahedral and octahedral sheets share apical oxygens, the lateral dimensions of both tetrahedral and octahedral sheets should be similar. All of the octahedral sites in talc are occupied so that the tetrahedra cannot significantly tilt out of the basal plane; this makes the basal oxygens nearly coplanar. Any change in composition in the octahedral sheet usually increases the lateral dimension of the octahedral layer. Such octahedral "thinning" is not enough to accommodate the distortions in the tetrahedral sheet, which reduces its lateral dimension by in-plane tilting of adjacent tetrahedra.^{39,40} The b dimension of the unit cell is more sensitive to the composition of the octahedral sheet than are the a and c dimensions. The position of the (060) reflection varies somewhat for different minerals because $d(060)$ depends on cation and site occupancy in the octahedral sheet, and on the degree of tetrahedral tilt.⁴¹ The value of $d(060)$ has been used to differentiate between trioctahedral and dioctahedral layered silicates⁴¹ as well as to estimate composition.¹⁹ In determining the composition of fluorotalc prepared using fluoride buffers, Duffy and Greenwood related the mole fraction of the fluoride end-member (x) to $d(060)$ using

eq 1:¹⁹

$$d(060) \text{ (in } \text{\AA}) = 1.52731 - 0.00615x \quad (1)$$

A similar linear relationship has been noted between $d(060)$ and fluoride substitutions between $\sim 10\%$ and $\sim 70\%$ in talc, prepared by a diphasic sol method and fired with a stoichiometric amount of water.^{23,24} Using eq 1 for product **3**, for which $d(060)$ was 1.52295 \AA , the fluoride substitution was calculated to be 71%, which agrees with the results of chemical analysis (see above).

Vibrational Analysis. The vibrational spectra of talc may be divided into regions that correlate with the O-H and Si-O stretching and bending vibrations. The IR spectra (Figure 6) of the synthetic fluorotalcs show a sharp, weak band between 3666 and 3671 cm^{-1} due to O-H stretching vibrations.^{40,42} A decrease in the O-H stretching frequency is observed for fluorotalc, compared to the hydroxylated talc for which $\nu(\text{O-H})$ is at 3676.8 cm^{-1} . The decrease in the O-H stretching frequency with increase in fluoride substitution was reported previously.²² The broad bands centered near 3500 and 1600 cm^{-1} are assigned to adsorbed water⁴³ on the surface of crystallites. $\nu(\text{O-H})$ for the nominally 90 and 100% substituted fluorotalcs (**4** and **6**, respectively, see Table 1) occurs at 3669 cm^{-1} , the same frequency as seen for **3**. This coincidence suggests that the talc phase that formed, along with MgF_2 , may be $\sim 70\%$ fluoride substituted.

The $\perp\nu_{\text{as}}(\text{Si-O-Si})$ stretching frequency for the fluoride-substituted talcs was observed at ~ 1040

(39) Evans, B. W.; Guggenheim, S. In *Hydrous Phyllosilicates (Exclusive of Micas)*, Bailey, S. W., Ed.; Mineralogical Society of America: Chelsea, Michigan, 1991, pp 225-294.

(40) Lazarev, A. N. *Vibrational Spectra and Structure of Silicates*; Consultants Bureau: New York, 1972.

(41) Moore, D. M.; R. C. Reynolds, J. *X-ray Diffraction and the Identification and Analysis of Clay Minerals*; Oxford University Press: Oxford, England, 1989; p 332.

(42) Farmer, V. C.; Russel, J. D. *Spectrochim. Acta* **1964**, *20*, 1149-1173.

(43) Little, L. H. *Infrared Spectra of Adsorbed Species*; Academic Press: London, 1966; p 233.

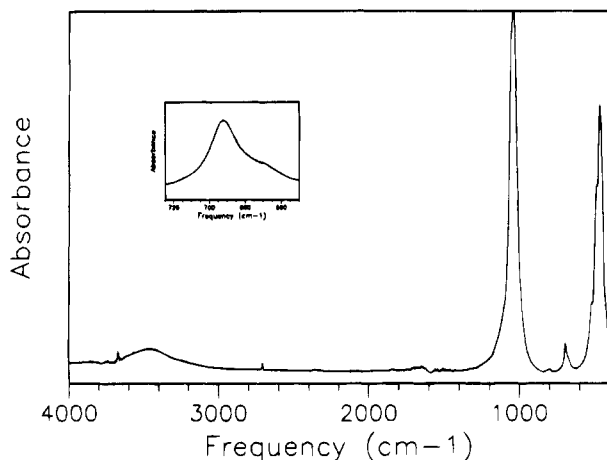


Figure 6. FTIR spectrum of 71% F-substituted talc, **3**. The inset shows the bands due to $\text{Mg}\delta(\text{OH})$ librations (670 cm^{-1}) and perpendicular Si–O vibration (690 cm^{-1} , sh). The sharp, weak band at 2706.3 cm^{-1} is due to talc's O–D stretching vibration (from D_2O that leaked into the reaction tube).

cm^{-1} .^{40,44} However, the band assigned to $\nu_{\text{as}}(\text{Si}-\text{O}-)$, which is expected at $\sim 1018\text{ cm}^{-1}$,⁴¹ is not usually seen in the fluoridated samples. Si–O bending vibrations were also observed between 400 and 600 cm^{-1} .

Natural (hydroxy) talc shows a band at $\sim 670\text{ cm}^{-1}$ with a shoulder at about 690 cm^{-1} . From inelastic neutron scattering studies and examination of O–D stretching vibrations of deuterated samples, the band at 670 cm^{-1} was assigned to $\text{Mg}\delta(\text{OH})$ librations.^{45,46} The shoulder at 690 cm^{-1} was assigned to perpendicular $\nu(\text{Si}-\text{O})$ vibrations.^{39,40,45,46} In contrast, the fluorotalcs have the band at 690 cm^{-1} as the more intense absorption with a shoulder at 670 cm^{-1} . This change in intensity is consistent with the decrease in the number of $\text{Mg}-\text{OH}$ bonds due to the substitution of OH by F.

Thermal Stability. The thermal decomposition of talc has been studied extensively.⁴⁷ Natural talc decomposes endothermically with loss of constitutional water (i.e., bound OH groups) between 800 and $850\text{ }^\circ\text{C}$. Synthetic talc without fluoride shows a maximum rate of this endotherm at $860\text{ }^\circ\text{C}$.²⁰ This temperature may be considered the upper limit of the thermal stability of talc. Talc with 50% fluoride substitution is reported to have an endothermic double peak at 1070 and $1085\text{ }^\circ\text{C}$, which was assigned to the release of hydroxide and possibly fluoride ions.²⁰ Thus, substitution of one-half of the hydroxides by fluoride increased the upper limit of thermal stability by 210 – $225\text{ }^\circ\text{C}$. An exotherm at $1230\text{ }^\circ\text{C}$ has been assigned to the crystallization of MgF_2 , cristobalite, and enstatite, and endotherms at 1250 and $1290\text{ }^\circ\text{C}$ were attributed to the loss of F from MgF_2 .²⁰

As shown in Figure 7, thermal analysis (TG and DTA) of **3**, the 71% F-substituted talc, heated under a flow of dry N_2 had an endotherm at $1075\text{ }^\circ\text{C}$ followed by a broad exotherm at $\sim 1125\text{ }^\circ\text{C}$. The maximum rate of weight loss, which occurs at $1075\text{ }^\circ\text{C}$, coincides with the endotherm and is $215\text{ }^\circ\text{C}$ higher than that of synthetic talc without fluoride.²⁰ This upper limit of thermal

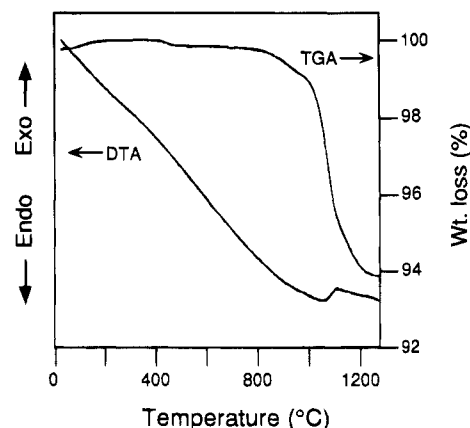


Figure 7. Thermogravimetric and differential thermal analysis of F-substituted talc, **3**, fired under a flow of dry N_2 ; the heating rate was $10\text{ }^\circ\text{C}/\text{min}$.

stability is similar to that, viz., $1096\text{ }^\circ\text{C}$, reported for a 68% fluoride substituted talc, which was prepared by a diphasic sol–gel route.^{22–24} XRD analysis showed that after heating at $1060\text{ }^\circ\text{C}$, the layer structure was still largely intact. However, broadening of the major peaks, the loss of some fine features, and the emergence of new peaks indicate that some decomposition had occurred. XRD analysis of the product after firing at $1300\text{ }^\circ\text{C}$ showed broad peaks at $\sim 28, 31, 36, 46,$ and $62\text{ }^\circ(2\theta)$ that are assigned to enstatite;⁴⁸ peaks from cristobalite⁴⁹ were absent.

Thermal analysis of the 45% F-substituted talc, **1**, showed maxima in the weight loss and in the endotherm at $1115\text{ }^\circ\text{C}$. This upper limit for thermal stability is $\sim 30\text{ }^\circ\text{C}$ higher than that reported by Van Valkenberg for 50% F-substituted talc.²⁰ Above this temperature, the TG slope was less steep, and the DTA trace showed a broad exotherm that may correspond to the crystallization of enstatite. XRD peaks at $28, 31, 33, 35.5, 46,$ and $62\text{ }^\circ(2\theta)$, matching those of enstatite,⁴⁸ were observed from the powder heated to $1200\text{ }^\circ\text{C}$; the characteristic peak of talc at $\sim 9^\circ$ was absent. Two other endotherms at 1289 and $1309\text{ }^\circ\text{C}$ corresponded to a third region of weight loss. The XRD pattern of powder heated to $1400\text{ }^\circ\text{C}$ showed additional peaks, including one at $\sim 22^\circ$, assigned to cristobalite.⁴⁹

Our observations agree well with the reported thermal behavior of talc for which decomposition was reported to proceed by simultaneous dehydration and crystallization of enstatite and silica.³⁹ However, XRD analysis of the thermal decomposition products of **1** and **3** showed no peak patterns that match those of MgF_2 .²⁰ Loss of fluoride ions as volatile decomposition products such as HF, which might form by reaction of $\text{Mg}-\text{F}$ groups with water or $\text{Mg}-\text{OH}$ groups, probably occurred since the observed weight losses are greater than those expected from loss of water alone. In both cases, fluoride substitution increased the decomposition temperatures by at least $198\text{ }^\circ\text{C}$ compared to talc without fluoride.

The lower decomposition temperature of **3** compared to **1** may indicate that too high a level of substitution may start to destabilize the talc structure. Other factors that may account for this observation, i.e., differences in particle size and crystallinity may be ruled out.

(44) Rosasco, G. J.; Blaha, J. J. *J. Appl. Spectrosc.* **1980**, *34*, 140–144.

(45) Naumann, A. W.; Safford, G. J.; Mumpton, F. A. *Clays Clay Miner.* **1966**, *14*, 367–383.

(46) Russell, J. D.; Farmer, V. C.; Velde, B. *Mineral. Mag.* **1970**, *37*, 869–879.

(47) Wesolowski, M. *Thermochim. Acta* **1984**, *78*, 395–421.

(48) Smith, J. V. *Acta Crystallogr.* **1959**, *12*, 515–519.

(49) Wong-Ng, W.; McMurdie, H.; Paretzkin, B.; Hubbard, C.; Drago, A. *Powder Diffraction* **1988**, *3*, 253.

Variations in transformation temperature observed by DTA have been attributed to crystallinity, instead of particle size; poorly crystallized phases are characterized by a shifting of reaction peaks to lower temperatures.⁵⁰⁻⁵⁴ In our case, however, the more crystalline material (see below), **3**, showed a lower decomposition temperature.

Water as a Mineralizer. The effect of water on the crystallization of silicates has been described.^{55,56} In the synthesis of illite from gels, for instance, a high water to solids ratio is necessary to get well crystallized products.⁵⁷ The mineralizing effect of water was quite evident in the degree of crystallization and the hardness of the fluorotalc products. For example, the product of a 100% F-substituted xerogel precursor fired without added water (**5**, see Table 1) was quite hard. The XRD pattern of **5** showed mainly weak, broad peaks at ~ 40 , 53 , and 63° (2θ) and gave no evidence of a layered structure. With added water, however, a soft, slippery powder was obtained; XRD analysis of **6** indicated the presence of talc as the major product. Depending on the presence or absence of water during firing, there was a significant difference in crystallinity of the products obtained from a xerogel precursor having nominally 75% F substitution. Although the presence of a peak near 9° (2θ) in the XRD patterns of **2** and **3** in Figure 8 show that a layered silicate formed in both cases, the narrowness of the peaks from the softer **3**, formed with added water, indicates that it is much more crystalline. Furthermore, the XRD pattern of **2** shows the presence of side products that may include norbergite, as seen from the peaks at ~ 29 , 34 , 40 , and 53° (2θ).³⁵ The XRD pattern of **1**, fired with no added water, had narrow peaks indicating a high degree of crystallinity, yet the powder was hard enough to pull metal from the walls of the reaction tubes upon removal. It is interesting to note that, qualitatively, the product's hardness seems to increase with increasing fluoride substitution in the experiments carried out under dry conditions.

Summary and Conclusions

Fluoridated talc with fluoride for hydroxyl substitution of up to 71% was synthesized at 750°C under a confining pressure of ~ 175 MPa from a xerogel prepared from a fluoridated magnesium silicate sol. Water, possibly acting as a mineralizer, appears to be necessary for the formation of a soft product. DTA analysis showed that the talc phase with 45% F substitution decomposes at 1115°C , representing a 255°C increase

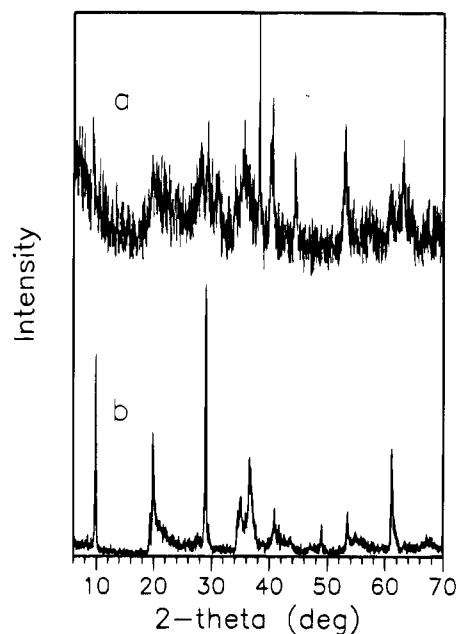


Figure 8. Comparison of XRD patterns of fluorotalc from a xerogel having a target F-substitution of 75% fired: (a) dry, **2**, and (b) with water added, **3**.

in the upper limit of thermal stability of synthetic talc without fluoride. The slightly lower decomposition temperature of the 71% F-substituted talc (1075°C) and the formation of MgF_2 when higher substitutions were attempted may indicate that too high a level of fluoride substitution may destabilize the structure.

The pressure used for synthesis of fluorotalc is considerably higher than that used for the preparation of fiber-reinforced ceramic matrix composites, and in situ formation of fluorotalc may not be practical. Whether fluorotalc will form at substantially lower pressures remains to be determined. Perhaps more importantly, the upper limit of thermal stability of fluorotalc is not high enough for most applications of CMCs.

Attempts to synthesize 90 and 100% fluoride substituted talc from xerogels with stoichiometric fluoride content yielded mixtures of a fluorotalc phase and MgF_2 . The similarity of the O-H stretching vibration of the former to that of 71% F-substituted talc suggests that fluoride ions do not fully substitute for hydroxide groups in the talc structure under the conditions used.

Acknowledgment. We thank the Office of Naval Research and DARPA for the major portion of the financial support, the MRL Program of NSF (Award No. DMR-9121654) for additional support and the NSF (CHE7904825; PGM8018643), NIH (RR02002), and IBM Corp. for helping provide NMR facilities in the Department of Chemistry. We also acknowledge many helpful discussions with Drs. Kenneth Chyung and Steven Dawes and Prof. David L. Kohlstedt.

CM950134P

(50) Bayliss, P. *Nature* **1964**, *201*, 1019.

(51) Smothers, W. J.; Chiang, Y. *Handbook of Differential Thermal Analysis*; Chemical Publishing Company, Inc.: New York, 1966; p 58.

(52) Caillere, S.; Henin, S. *Verre Silicates Ind.* **1947**, *12*.

(53) Caillere, S.; Henin, S. *Compt. Rend.* **1947**, *224*, 1439-40.

(54) Arens, P. L. *Soil Sci.* **1951**, *72*, 406.

(55) Laudise, R. A. *Chem. Eng. News* **1987**, *Sept 28*, 30-43.

(56) Buerger, M. J. *Am. Miner.* **1948**, *33*, 744-747.

(57) Eberl, D.; Hower, J. *U. S. Geol. Soc. Bull.* **1976**, *87*, 1326-1330.